

- [6] R. A. Giordano, B. M. Wu, S. W. Borland, L. Griffith-Cima, E. M. Sachs, M. J. Cima, *J. Biomater. Sci., Polym. Ed.* **1996**, *8*, 63.
- [7] J. T. Borenstein, H. Terai, K. R. King, E. J. Weinberg, M. R. Kaazempur-Mofrad, J. P. Vacanti, *Biomed. Microdevices* **2002**, *4*, 167.
- [8] S. Kaihara, J. T. Borenstein, R. Koka, S. Lalan, E. R. Ochoa, M. Ravens, H. Pien, B. Cunningham, J. P. Vacanti, *Tissue Eng.* **2000**, *6*, 105.
- [9] C. Fidkowski, M. R. Kaazempur-Mofrad, J. T. Borenstein, J. P. Vacanti, R. Langer, Y. Wang, *Tissue Eng.* **2005**, *11*, 302.
- [10] E. Leclerc, S. Yasuyuki, T. Fujii, *Biomed. Microdevices* **2003**, *5*, 109.
- [11] M. J. Powers, K. Domansky, M. R. Kaazempur-Mofrad, A. Kalezi, A. Capitano, A. Upadhyaya, P. Kurzawski, K. E. Wack, D. B. Stolz, R. Kamm, L. G. Griffith, *Biotechnol. Bioeng.* **2002**, *78*, 257.
- [12] E. Leclerc, Y. Sakai, T. Fujii, *Biotechnol. Prog.* **2004**, *20*, 750.
- [13] K. R. King, C. C. J. Wang, M. R. Kaazempur-Mofrad, J. P. Vacanti, J. T. Borenstein, *Adv. Mater.* **2004**, *16*, 2007.
- [14] D. H. Leatrese, B. S. Kim, D. J. Mooney, *J. Biomed. Mater. Res.* **1998**, *42*, 396.
- [15] Y. Wang, G. A. Ameer, B. J. Sheppard, R. Langer, *Nat. Biotechnol.* **2002**, *20*, 602.
- [16] Y. Wang, Y. M. Kim, R. Langer, *J. Biomed. Mater. Res., Part A* **2003**, *66*, 192.
- [17] A. A. Ignatius, L. E. Claes, *Biomaterials* **1996**, *17*, 831.
- [18] C. A. Sundback, J. Y. Shyu, Y. Wang, W. C. Faquin, R. S. Langer, J. P. Vacanti, T. A. Hadlock, *Biomaterials* **2005**, *26*, 5454.
- [19] D. C. Duffy, J. C. McDonald, J. A. Schueller, G. M. Whitesides, *Anal. Chem.* **1998**, *70*, 4974.
- [20] E. Clementi, G. C. Brown, N. Foxwell, S. Moncada, *Proc. Natl. Acad. Sci. USA* **1999**, *96*, 1559.
- [21] N. Resnick, H. Yahav, A. Shay-Salit, M. Shushy, S. Schubert, L. Zilberman, E. Wofovitz, *Prog. Biophys. Mol. Biol.* **2003**, *81*, 177.
- [22] C. F. Dewey, S. R. Bussolari, M. A. Gimbrone, P. F. Davies, *J. Biomech. Eng.* **1981**, *103*, 177.
- [23] A. M. Malek, S. Izumo, *Am. J. Physiol.* **1992**, *263*, C389.
- [24] F. P. Incropera, D. P. Dewitt, *Fundamentals of Heat and Mass Transfer*, Wiley, New York **2002**.
- [25] E. G. Clementi, G. C. Brown, N. Foxwell, S. Moncada, *Proc. Natl. Acad. Sci. USA* **1999**, *96*, 1559.
- [26] C. D. Collard, A. Agah, G. L. Stahl, *Immunopharmacology* **1998**, *39*, 39.
- [27] E. J. Weinberg, J. T. Borenstein, M. R. Kaazempur-Mofrad, B. Orrick, J. P. Vacanti, *Mater. Res. Soc. Symp. Proc.* **2004**, *820*, 121.
- [28] D. P. Aden, A. Fogel, S. Potkin, I. Damjanov, B. B. Knowles, *Nature* **1979**, *282*, 615.
- [29] J. H. Kelly, *US Patent 5 290 684*, **1994**.
- [30] F. Re, A. Zanetti, M. Sironi, N. Polentarutti, L. Lanfrancone, E. Dejana, F. Colotta, *J. Cell Biol.* **1994**, *127*, 537.
- [31] S. Cereghini, M. Blumenfeld, M. Yaniv, *Genes Dev.* **1988**, *2*, 957.
- [32] D. M. Richardson, M. C. Peters, A. B. Ennet, D. J. Mooney, *Nat. Biotechnol.* **2001**, *19*, 1029.
- [33] K. Y. Suh, J. Seong, A. Khademhosseini, P. E. Laibinis, R. Langer, *Biomaterials* **2001**, *25*, 557.
- [34] A. Khademhosseini, K. Y. Suh, J. M. Yang, G. Eng, J. Yeh, S. Levenberg, R. Langer, *Biomaterials* **2004**, *25*, 3583.
- [35] R. F. Flemming, C. J. Murphy, G. A. Abrams, S. L. Goodman, P. F. Nealey, *Biomaterials* **1999**, *20*, 573.
- [36] S. N. Bhatia, U. J. Balis, M. L. Yarmush, M. Toner, *FASEB J.* **1999**, *13*, 1883.
- [37] R. M. Sok, *Ph.D. Thesis*, University of Groningen, The Netherlands **1994**.

DOI: 10.1002/adma.200501639

Organic Light-Emitting Transistors Based on Solution-Cast and Vacuum-Sublimed Films of a Rigid Core Thiophene Oligomer**

By Fabio Cicoira,* Clara Santato, Manuela Melucci, Laura Favaretto, Massimo Gazzano, Michele Muccini, and Giovanna Barbarella

Organic thin films have been widely investigated as active layers in electronic and optoelectronic devices, such as field-effect transistors (FETs), light-emitting diodes (LEDs), and photovoltaic cells.^[1]

The recent fabrication of organic light-emitting (field-effect) transistors (OLETs), a class of multifunctional devices that allow the integration of a light source with the typical switching function of a transistor, represents a very promising step for the development of highly integrated organic optoelectronic devices. After the first demonstration of OLETs employing a vacuum-sublimed tetracene film as an active layer,^[2] a number of devices have been reported. Polymer-based OLETs, where the active layer has been processed by spin coating, have been obtained from poly(9,9-diethylhexylfluorene)^[3] and poly[2-methoxy-5-(2'-ethylhexyloxy)-1,4-phenylenevinylene].^[4] A co-evaporated layer of α -quinoxithiophene (T5) and *N,N*-8-ditridecylperylene-3,4,9,10-tetracarboxylic diimide (P13) has been used to produce the first ambipolar OLET.^[5a] The approach has been demonstrated to be of general validity for tuning the transport and electroluminescence (EL) characteristics of OLETs.^[5b] The role played by the channel length has been investigated in OLETs based on a vacuum-sublimed film of 2,4-bis(4-(2'-

[*] Dr. F. Cicoira,^[+] Dr. C. Santato, Dr. M. Muccini
Consiglio Nazionale delle Ricerche (CNR)
Istituto per lo Studio dei Materiali Nanostrutturati (ISMN)
Via Gobetti 101, I-40129 Bologna (Italy)
E-mail: cicoira@bo.imm.cnr.it

Dr. M. Melucci, L. Favaretto, Dr. M. Gazzano, Dr. G. Barbarella
Consiglio Nazionale delle Ricerche (CNR)
Istituto per lo Studio della Sintesi Organica e la Fotoreattività (ISOF)
Via Gobetti 101, I-40129 Bologna (Italy)

[+] Present address: INRS-EMT Université du Québec, 1650, Boulevard Lionel Boulet, Varennes, Québec J3X 152, Canada.

[**] We acknowledge P. L. Bellutti (IRST, Trento) for the supply of patterned substrates, P. Doppelt and A. Mantoux (CNRS, Vitry, France) for substrate silylation, A. Bonfiglio and P. Cosseddu (INFM-S3 Modena and University of Cagliari) for AFM imaging, S. Toffanin (CNR/ISMN) for LSCM imaging, R. Zamboni (CNR/ISMN) for fruitful discussions, and F. Rosei and F. Pietropaolo for critical reading of the manuscript. Funding from projects EU-NMP IP 500355 NAIMO and FIRB-RBNE033KMA is kindly acknowledged.

thiophenyl)phenyl)thiophene (TPTPT).^[6] Finally, the possibility to extend OLET fabrication to plastic substrates has been shown for tetracene-based devices.^[7] The further development of OLETs requires the engineering and synthesis of novel multifunctional materials that combine good charge transport and efficient EL. In addition, since the interest in organic optoelectronics resides in the possibility to fabricate large-area and low-cost devices,^[8] the solubility of the organic semiconductor, which allows processing by casting and printing processes, is a paramount issue.

In this work, we report on the design, synthesis, thin-film growth, and optoelectronic properties of the newly synthesized dithienothiophene derivative 2,6-bis-(5'-hexyl-[2,2']bithiophen-5-yl)-3,5-dimethyl-dithieno[3,2-*b*;2',3'-*d*]thiophene (DTT7Me), whose structure is shown in Scheme 1. DTT7Me films, grown both by vacuum sublimation and, more importantly for technological applications, by drop casting, were successfully employed as active layers in OLETs.

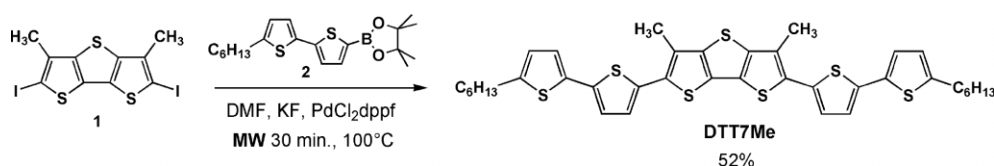
DTT7Me was synthesized by microwave-assisted Suzuki coupling,^[9] as shown in Scheme 1, and purified by means of repeated washings with solvents of increasing polarity followed by crystallization from toluene. Unlike the unmethylated derivative,^[10] DTT7Me is a liquid crystalline compound.

In designing the DTT7Me molecule, our objective was to achieve the delicate balance of forces needed to obtain the supramolecular organization in solution-processed films that gives rise to both good charge transport and EL.^[11] Previous investigations on oligomers containing the dithienothiophene moiety indicated that such compounds can yield high hole FET mobilities.^[10,12] Strong photoluminescence (PL) as well as EL in a LED configuration was detected from thin films of dithienothiophene *S,S*-dioxide derivatives.^[13] The molecular structure of DTT7Me can be viewed as a hexyl-terminated sexithiophene in which the two central rings are rigidly held by an additional sulfur. The presence of the two methyl substituents enhances solubility^[13b] and keeps molecules in the solid state sufficiently far apart to prevent PL quenching. In agreement with this, preliminary measurements indicate that the DTT7Me crystalline powder has a PL quantum yield higher than its unmethylated counterpart. The terminal hexyl chains are expected to increase the structural order of the film and thus enhance charge transport.^[14] Being thermally stable and soluble in organic solvents, DTT7Me offers the interesting opportunity to grow films by solution processes, to enable comparison with vacuum-sublimed films.

To gain an insight into the growth mode and the surface morphology of vacuum-sublimed DTT7Me films, we analyzed films having a nominal thickness of 3, 6, and 20 nm by atomic

force microscopy (AFM) (Figs. 1a–c, respectively). Films were grown with a nominal deposition flux (F) of 0.4 \AA s^{-1} on an SiO_2 dielectric. Figure 1a shows that DTT7Me has an island-type growth on SiO_2 . The islands have a uniform spatial distribution with an average density of $20 \mu\text{m}^{-2}$ and a typical size of 80 nm. Increasing the nominal thickness to 6 nm results in coalescence of the islands, which leads to the formation of an almost continuous film whose grains have an elongated shape. A further increase of the nominal thickness to 20 nm leads to complete substrate coverage and to an increase of domain size. The results reveal that DTT7Me has a good adhesion to SiO_2 and that low nominal thicknesses are sufficient to form continuous films. Laser scanning confocal microscopy (LSCM) images of a vacuum-sublimed and a drop-cast DTT7Me film are shown in Figures 1d,e, respectively. Within the resolution limit of LSCM, a spatially uniform luminescence signal is observed for vacuum-sublimed films, whereas the drop-cast film shows spatial inhomogeneity, which is possibly due to high film roughness.

Figure 2 shows X-ray diffraction (XRD) patterns of DTT7Me films deposited on SiO_2 by a) vacuum sublimation and b) drop casting, together with c) the pattern of the DTT7Me precursor powder. This last pattern shows several peaks that are characteristic of a well-developed crystalline phase. Both cast and vacuum-evaporated films display a high degree of order. The profile of the cast film shows peaks already observed in the powder together with peaks that appear as high-order reflections that originate from the same family of planes. Reflections are detected at $2\theta = 5.4, 8.1, 10.8, 13.4,$ and 16.2° , which correspond to d -spacings of 1.64, 1.08, 0.83, 0.66, and 0.55 nm, thus suggesting an interplanar distance of ~ 3.3 nm. The presence of several high-order reflections confirms the high degree of orientation with respect to the substrate in the cast film. Further studies are in progress to determine the structure of the phase, to describe the molecular interactions stabilizing it, and to determine the orientation of the crystals. The pattern of the vacuum-sublimed film is characterized by two very narrow peaks. They are located at $2\theta = 3.6$ and 7.0° , which correspond to d -spacings of 2.45 and 1.26 nm and can be attributed to subsequent orders belonging to the same family of planes separated by 2.45 nm. The absence of these reflections in the powder profile is a confirmation that the two crystalline phases belong to different polymorphs. The structural organization of evaporated DTT7Me is not easily deduced from our X-ray diagram. One of the reasons of the polymorph differentiation could be a conformational change caused by the variation of the inter-ring angles. Nevertheless, by analogy to what was found in α,ω -dihex-



Scheme 1. Synthetic pattern for the preparation of DTT7Me. DMF: dimethylformamide; dppf: diphenylphosphinoferrocene.

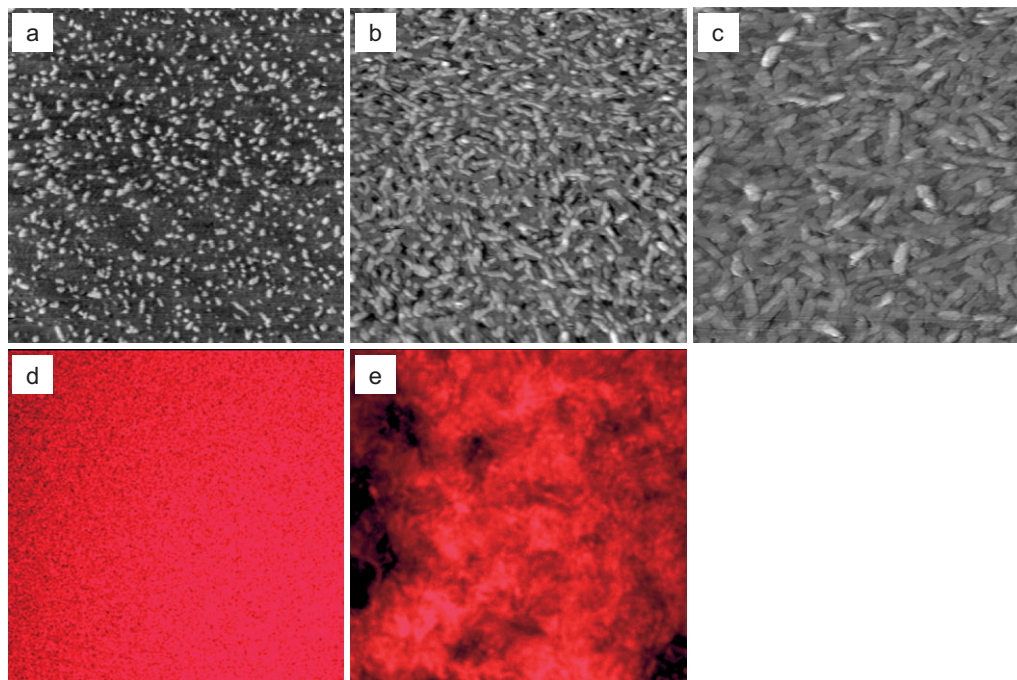


Figure 1. AFM micrographs ($4.5 \mu\text{m} \times 4.5 \mu\text{m}$) of DTT7Me films grown on SiO_2 at a nominal deposition flux of 0.4 \AA s^{-1} having nominal thicknesses of a) 3, b) 6, and c) 20 nm. The root-mean-square roughnesses of the films are 1.4, 1.9, and 2.5 nm, respectively. Laser scanning confocal microscopy (LSCM) fluorescence images ($100 \mu\text{m} \times 100 \mu\text{m}$) of d) a 20 nm thick vacuum-sublimed film and e) a drop cast film, on SiO_2 .

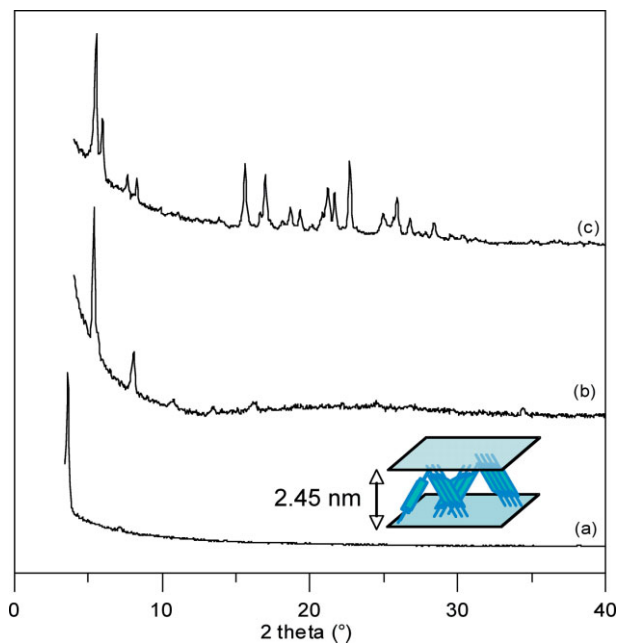


Figure 2. XRD pattern of DTT7Me: a) a 20 nm thick vacuum-sublimed film ($F=0.4 \text{ \AA s}^{-1}$) on SiO_2 ; b) a cast film on SiO_2 , and c) the precursor powder.

ylthiophenes,^[13a] we hypothesize the following picture (see inset, Figure 2). If a molecule length for DTT7Me of about 3.7 nm (extended conformation) is assumed, and the lateral hexyl chains do not overlap, the reflections would indicate an

angle of about 45° between the DTT7Me molecules and the substrate normal. Therefore, it is suggested that the sublimed film results from layers formed by a unique domain of iso-oriented molecules or from different domains that do not coincide in their relative orientations.

To optimize FET mobility and to determine the minimum thickness needed to achieve charge transport, several DTT7Me-based organic field-effect transistors (OFETs) were fabricated with the active-layer thickness varying in the range 6–25 nm, at a deposition flux of 0.4 \AA s^{-1} . In agreement with the AFM micrographs mentioned above, electrical measurements show that an active-layer thickness of 6 nm is sufficient to obtain a working FET. In addition, the active-layer thickness does not significantly affect the FET characteristics. This result is explained by charge transport occurring mainly at the organic/dielectric interface.^[15] The typical hole FET mobility, from about 15 devices obtained in different deposition runs, is $\sim 2 \times 10^{-2} \text{ cm}^2 \text{ V}^{-1} \text{ s}^{-1}$.

DTT7Me active layers, grown both by vacuum sublimation and drop casting from a DTT7Me solution in toluene, were successfully employed in the fabrication of light-emitting transistors. Films were grown on bottom-contact Au source–drain electrodes that were ring-shaped to circumvent parasitic currents due to the unpatterned semiconductor layer.^[16] To ensure charge injection from Au, a molecular 3-mercaptopropyl trimethoxysilane (MPTMS) adhesion layer was used between the electrodes and the SiO_2 gate dielectric, instead of the commonly employed metallic adhesion layers.^[17] The output optoelectronic characteristics of OLETs that employed vacu-

um-sublimed and drop-cast active layers are shown in Figures 3a,b, respectively. The plots report drain-source current (I_{ds}) on the left y-axis and EL on the right y-axis, as a function of the drain-source voltage (V_{ds}), at increasing gate-source voltages (V_{gs}). The I_{ds} - V_{ds} plots show that DTT7Me-based devices behave as unipolar *p*-type FETs working in accumulation mode (no electronic transport was detected under a positive V_{gs} bias). I_{ds} rapidly increases for low V_{ds} and then attains a saturation regime ($I_{ds,sat}$) for larger V_{ds} . The I_{ds} current at saturation increases quadratically with V_{gs} . The FET mobility (μ) was extracted in the saturation regime by using the relation:

$$|I_{ds,sat}| = \frac{W}{2L} \mu C_i (V_{gs} - V_T)^2 \quad (1)$$

where W and L are the channel width and length, respectively, C_i is the gate dielectric capacitance per unit area

($1.8 \times 10^{-8} \text{ F cm}^{-2}$ for 190 nm thick SiO_2), and V_T is the threshold voltage deduced from the intercept at $y=0$ of the ($|I_{ds,sat}|$)^{1/2} vs. V_{gs} plot.^[18] The FET characteristics depend on the method of deposition of the active layer. Indeed, for a vacuum-sublimed film, μ is $\sim 2 \times 10^{-2} \text{ cm}^2 \text{ V}^{-1} \text{ s}^{-1}$, $V_T \sim -10 \text{ V}$, and $I_{on}/I_{off} \sim 10^6$ (calculated from transfer curves at $V_{ds} = -70 \text{ V}$ taking I_{off} at $V_{gs} = 0 \text{ V}$ and I_{on} at $V_{gs} = -70 \text{ V}$). For solution-processed devices, μ is $\sim 1 \times 10^{-2} \text{ cm}^2 \text{ V}^{-1} \text{ s}^{-1}$, V_T is 10 V and I_{on}/I_{off} is ~ 10 . The lower mobility compared with sublimed films, and the observation of a positive threshold voltage are probably due to a lack of complete control of the drop-cast process and/or to a different crystal structure of the film.

The most striking feature in Figure 3 is that both sublimed and cast layers are able to generate EL in the FET configuration under an appropriate bias. The optical output characteristics are quite similar in the two differently processed devices.

The onset of EL, for a fixed V_{gs} , occurs at more negative drain-source voltages than the onset of I_{ds} . The EL continuously increases with increasing $|V_{ds}|$, and also increases with $|V_{gs}|$. The minimum $|V_{gs}|$ value needed to detect light emission is $\sim -10 \text{ V}$. Work is in progress to understand the nature of the fundamental excitations responsible for the EL together with the evolution of the EL spectra as a function of the preparation of the active layer. The external quantum efficiency (i.e., the number of photons emitted per electron flowing in the device, EQE) of DTT7Me-based OLETs is comparable with that reported for tetracene-based OLETs.^[19] As DTT7Me is a novel material, we strongly believe that the optoelectronic performance of the devices can be improved upon optimization of the active-layer growth together with substrate processing and surface treatment. In agreement with what was previously observed with tetracene-based OLETs, the EQE increases linearly with increasing $|V_{ds}|$ whereas it is constant with increasing $|V_{gs}|$.^[19] Electron injection from Au into the DTT7Me-based OLET is most probably an energetically unfavorable process (based on reports of the highest occupied molecular orbital/lowest unoccupied molecular orbital energy levels of the DTT7Me unmethylated counterpart by Iosip et al.^[10]). Nevertheless, the observation of the EL indicates that both electrons and holes are injected in the device. The unipolar nature of the charge transport in the

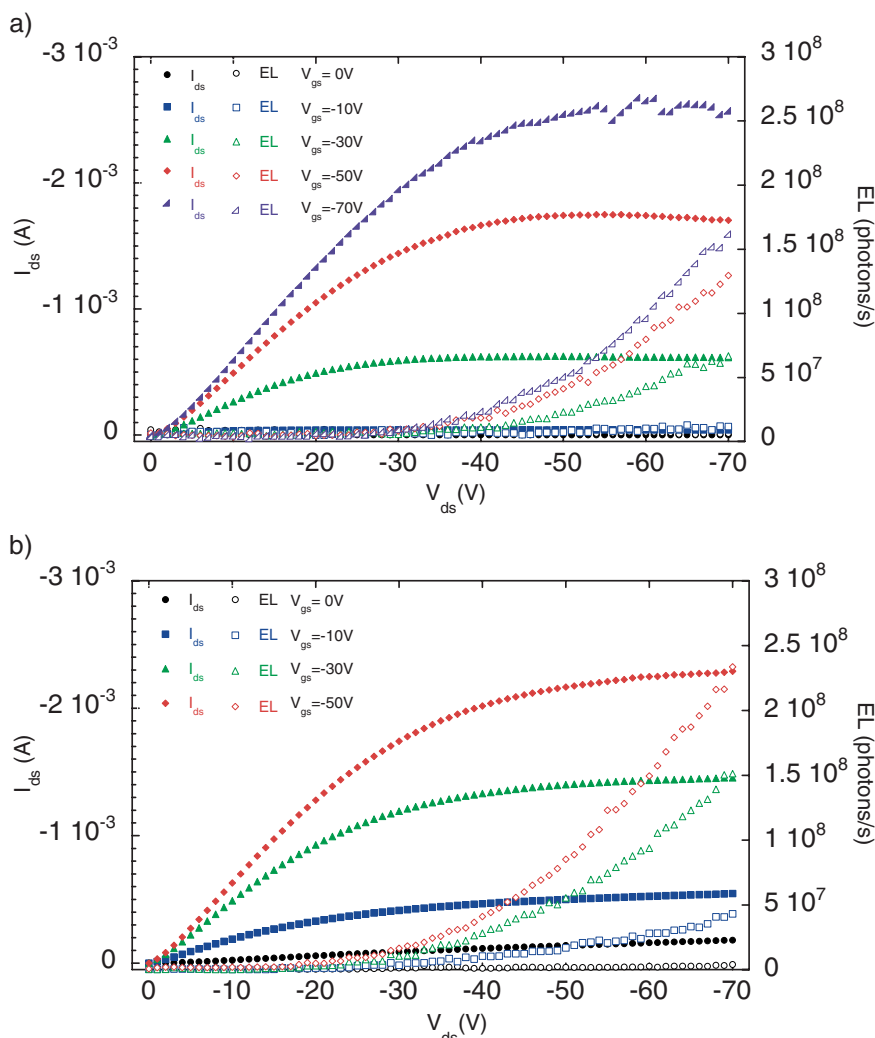


Figure 3. Optoelectronic output characteristics of DTT7Me-based OLETs. Drain-source current (I_{ds}) on the left y-axis, and EL on the right y-axis, vs. drain-source voltage (V_{ds}), recorded at various gate-source voltages (V_{gs}). a) Vacuum-sublimed film (thickness 20 nm, $F = 0.4 \text{ \AA}^{-1} \text{ s}^{-1}$), $W/L = 42\,000/10$ ($\mu\text{m}/\mu\text{m}$). b) drop cast film, $W/L = 42\,000/6$ ($\mu\text{m}/\mu\text{m}$); W = channel width, L = channel length.

DTT7Me-based OLET suggests that the EL is located close to the contact where the low mobility charge carriers are injected. If we assume that the EL intensity is mainly determined by the number of minority carriers (electrons) injected in the active layer, the similarity in optical properties the two different devices exhibit in terms of EL intensity is not surprising, since they are based on active layers made up of the same molecule and use the same Au electrodes. The topic of electron injection and transport in FET devices based on organic thin films is, nowadays, a matter of deep investigation and open debate.^[2,6,19,20] The collection of experimental results from OLETs employing different active materials, gate dielectrics, electrodes, as well as different device geometries, could be extremely helpful for a deeper understanding of this topic.

In conclusion, we report on the design and synthesis of a new organic multifunctional material, DTT7Me, a rigid core thiophene oligomer. AFM and LSCM images show that both vacuum-sublimed and drop-cast DTT7Me films have good SiO₂ surface coverage. XRD reveals that the films have a highly ordered structure. Of great interest for future technological applications, OLETs were successfully fabricated by not only vacuum sublimation but also drop casting. Our results introduce several novelties in organic optoelectronics both from a fundamental and practical point of view: the demonstration of a novel multifunctional material able to conjugate good charge transport and EL in a FET configuration, and the first solution-processed OLET based on non-polymeric systems. This last result, combined with the recent demonstration of OLETs on plastic substrates,^[7] paves the way towards all-plastic, low-temperature processed, large-area organic optoelectronics.

Experimental

Synthesis of Materials: A PdCl₂(diphenylphosphinoferrocene) complex with CH₂Cl₂, KF, 5-hexyl-5'-(4,4,5,5-tetramethyl-1,3,2-dioxaborolan-2-yl)-2,2'-bithiophene (compound 2) and *N*-iodosuccinimide (NIS) were commercial products. All solvents were used without further purification. Microwave-assisted reactions were carried out in air using a commercial system Synthwave 402, with variable power and fixed temperature. 3,5-Dimethyl-2,6-diiodo-dithieno[3,2-*b*:2',3'-*d*]thiophene (compound 1) was prepared using NIS and following already described procedures [21].

2,6-Bis-(5'-hexyl-[2,2']bithiophen-5-yl)-3,5-dimethyl-dithieno[3,2-*b*:2',3'-*d*]thiophene (DTT7Me): The microwave oven reactor was charged with compound 1 (50 mg, 0.105 mmol), compound 2 (199 mg, 0.53 mmol), Pd catalyst (4 mg, 5 mol-%), and KF (97 mg, 1.67 mmol) dissolved in 5 mL of dimethylformamide (DMF). The mixture was irradiated at 100 °C for 30 min. After cooling to room temperature the red precipitate was centrifuged at 2000 rpm and washed with H₂O, acetone, and finally with CH₂Cl₂. Crystallization from ligroin/toluene afforded DTT7Me as a deep red powder (40 mg, 52 % yield). Mp 267–269 °C, λ_{max} (CH₂Cl₂) = 423 nm, MS: *m/z* = 720 [M⁺], IR: 2954.4, 2922.4, 1431.5, 1381.8, 1070.4, 792.6, 778.1 cm⁻¹. ¹H NMR (CDCl₃): δ = 7.07 (br s, 4H), 7.02 (br d, *J* = 3.6 Hz, 2H), 6.69 (br d, *J* = 2.8 Hz, 2H), 2.80 (t, 4H), 2.53 (s, 6H), 1.71 (m, 4H), 1.33 (m, 12H), 0.90 (t, 6H). C₃₈H₄₀S₇ (720.12): Calcd. C 63.29, H 5.59; Found C 62.22, H 5.55. Differential scanning calorimetry (DSC) showed two well separated endothermic peaks at 183 °C (Δ*H* = 62 mJ) and at 272 °C (Δ*H* = 0.8 mJ).

Thin Film Deposition and Device Fabrication: Vacuum-sublimed films were grown using an apparatus already described elsewhere [15c]. Cast films were grown by dropping a 1.4 × 10⁻³ M solution of DTT7Me in warm toluene on a substrate held at 50 °C. For morphological analysis and XRD, films were deposited onto 190 nm thick SiO₂ thermally grown on heavily *n*-doped (Sb) Si. For electrical and optoelectronic characterizations, films were deposited onto the same type of substrates pre-patterned with ring-shaped, 30 nm thick Au source/drain bottom contacts. Prior to Au evaporation the SiO₂ surface was treated by MP-TMS [22]. The heavily doped *n*-Si substrate was used as a gate electrode. Devices had channel lengths of 6, 10, and 40 μm and corresponding channel widths of 42 000, 41 000, and 18 000 μm. Prior to deposition, substrates were cleaned by exposure to O₂ plasma (100 W power, for 5 min).

AFM Measurements: The film morphology was studied with a SPM Solver Pro AFM (NT-MDT) in tapping mode with NSG-01 Si cantilevers (NT-MDT).

Fluorescence Imaging: Fluorescence imaging of the samples was performed with a laser scanning confocal microscope (Nikon TE 2000) where fluorescence was excited at 488 nm with an Ar⁺ laser beam with controlled in-plane polarization.

XRD: XRD measurements were carried out by means of a Panalytical X'Pert Pro diffractometer system, equipped with a Cu anode as X-ray source. A parallel beam optic was used for thin film analysis (fixed glancing angle of 0.8°).

Optoelectronic Measurements: Optoelectronic measurements were carried out at room temperature under vacuum (10⁻³ Pa) with the OLETs placed in a probe station inside a calibrated integrating sphere where light detection was achieved through a pre-amplified photomultiplier [23]. All measurements were performed on freshly prepared samples.

Received: August 7, 2005

Final version: September 20, 2005

Published online: December 8, 2005

- a) F. Garnier, G. Horowitz, X. Peng, D. Fichou, *Adv. Mater.* **1990**, *2*, 592. b) P. Ostojia, S. Guerri, S. Rossini, M. Servidori, C. Taliani, R. Zamboni, *Synth. Met.* **1993**, *54*, 447. c) C. W. Tang, S. A. Van Slyke, *Appl. Phys. Lett.* **1987**, *51*, 913. d) J. H. Burroughes, D. D. C. Bradley, A. R. Brown, R. N. Marks, K. Mackay, R. H. Friend, P. L. Burns, A. B. Holmes, *Nature* **1990**, *347*, 539. e) N. S. Sariciftci, L. Smilowitz, A. J. Heeger, F. Wudl, *Science* **1992**, *258*, 1474.
- A. Hepp, H. Heil, W. Weise, M. Ahles, R. Schmechel, H. von Seggern, *Phys. Rev. Lett.* **2003**, *91*, 157406.
- M. Ahles, A. Hepp, R. Schmechel, H. von Seggern, *Appl. Phys. Lett.* **2004**, *84*, 428.
- T. Sakanoue, E. Fujiwara, R. Yamada, H. Tada, *Appl. Phys. Lett.* **2004**, *84*, 3037.
- a) C. Rost, S. Karg, W. Riess, M. A. Loi, M. Murgia, M. Muccini, *Appl. Phys. Lett.* **2004**, *85*, 1613. b) M. A. Loi, C. Rost-Bretsch, M. Murgia, S. Karg, W. Riess, M. Muccini, *Adv. Funct. Mater.* **2005**, in press.
- T. Oyamada, H. Sasabe, C. Adachi, S. Okuyama, N. Shimoi, K. Matsushige, *Appl. Phys. Lett.* **2005**, *86*, 093505.
- C. Santato, I. Manunza, A. Bonfiglio, F. Ciccoira, P. Cosseddu, R. Zamboni, M. Muccini, *Appl. Phys. Lett.* **2005**, *86*, 141106.
- S. R. Forrest, *Nature* **2004**, *428*, 911.
- M. Melucci, G. Barbarella, M. Zambianchi, P. Di Pietro, A. Bongini, *J. Org. Chem.* **2004**, *69*, 4821.
- M. D. Iosip, S. Destri, M. Pasini, W. Porzio, K. P. Pernstich, B. Batlogg, *Synth. Met.* **2004**, *146*, 251.
- E. Tedesco, F. Della Sala, L. Favaretto, G. Barbarella, D. Albesa-Jové, D. Pisignano, G. Gigli, R. Cingolani, K. D. M. Harris, *J. Am. Chem. Soc.* **2003**, *125*, 12277.
- X. C. Li, H. Sirringhaus, F. Garnier, A. B. Holmes, S. C. Moratti, N. Feeder, W. Clegg, S. J. Teat, R. Friend, *J. Am. Chem. Soc.* **1998**, *120*, 2206.

- [13] a) L. Antolini, E. Tedesco, G. Barbarella, L. Favaretto, G. Sotgiu, M. Zambianchi, D. Casarini, G. Gigli, R. Cingolani, *J. Am. Chem. Soc.* **2000**, *122*, 9006. b) G. Barbarella, L. Favaretto, G. Sotgiu, L. Antolini, G. Gigli, R. Cingolani, A. Bongini, *Chem. Mater.* **2001**, *13*, 4112.
- [14] a) F. Garnier, A. Yassar, R. Hajlaoui, G. Horowitz, F. Deloffre, B. Servet, S. Ries, P. Alnott, *J. Am. Chem. Soc.* **1993**, *115*, 8716. b) M. Halik, H. Klauk, U. Zschieschang, G. Schmidt, S. Pomarenko, S. Kirchmeyer, W. Weber, *Adv. Mater.* **2003**, *15*, 917.
- [15] a) F. Dinelli, M. Murgia, P. Levy, M. Cavallini, F. Biscarini, D. M. de Leeuw, *Phys. Rev. Lett.* **2004**, *92*, 116802. b) G. Horowitz, *Adv. Funct. Mater.* **2003**, *13*, 53. c) F. Cicaira, C. Santato, F. Dinelli, M. Murgia, M. A. Loi, F. Biscarini, R. Zamboni, P. Heremans, M. Muccini, *Adv. Funct. Mater.* **2005**, *15*, 375.
- [16] E. J. Meijer, C. Detcheverry, P. J. Baesjou, E. van Veenendaal, D. M. de Leeuw, T. M. Klapwijk, *J. Appl. Phys.* **2003**, *93*, 4831.
- [17] N. Yoneya, M. Noda, N. Hirai, K. Nomoto, M. Wada, J. Kasahara, *Appl. Phys. Lett.* **2004**, *85*, 4663.
- [18] S. M. Sze, *Physics of Semiconductor Devices*, 2nd Edition, Wiley, New York **1981**.
- [19] C. Santato, R. Capelli, M. A. Loi, M. Murgia, F. Cicaira, V. A. L. Roy, P. Stallinga, R. Zamboni, C. Rost, S. Karg, M. Muccini, *Synth. Met.* **2004**, *146*, 329.
- [20] a) R. H. Friend, R. W. Gymer, A. B. Holmes, J. H. Burroughes, R. N. Marks, C. Taliani, D. D. C. Bradley, D. A. Dos Santos, J. L. Brédas, M. Lögdlund, W. R. Salaneck, *Nature* **1999**, *397*, 121. b) L. L. Chua, J. Zaumseil, J. F. Chang, E. C. W. Ou, P. K. H. Ho, H. Sirringhaus, R. H. Friend *Nature* **2005**, *434*, 194.
- [21] F. De Jong, M. J. Janssen, *J. Org. Chem.* **1971**, *36*, 1645.
- [22] P. Doppelt, N. Semaltianos, C. Deville Cavellin, J. L. Pastol, D. Bal-lutaud, *Microelectron. Eng.* **2004**, *76*, 113.
- [23] P. Mei, M. Murgia, C. Taliani, E. Lunedei, M. Muccini, *J. Appl. Phys.* **2000**, *88*, 5158.

DOI: 10.1002/adma.200500913

Highly Periodic Fullerene Nanomesh**

By Nicolas Néel, Jörg Kröger,* and Richard Berndt

The last decade has witnessed many efforts to realize parallel fabrication of long-range-ordered nanostructures on surfaces. The controlled fabrication of highly periodic metal,^[1] semiconductor,^[2,3] or molecular^[4] nanostructures at surfaces remains, however, a challenging endeavor in nanoscience research. Large quantities of structures can be created in parallel by self-organized growth, either in the kinetic,^[5] or thermodynamic regime,^[2,3,6] and deposition of size-selected clus-

ters from the gas phase.^[7] Owing to the statistical nature of deposition and diffusion processes it is difficult to achieve lateral order by this approach. Consequently, prestructured samples have been studied intensely to enhance ordering on a large scale. On planar surfaces, for instance, the use of strained layers and dislocations as templates for subsequent depositions leads to self-organization over several dozens of nanometers.^[1] Supramolecular surface assemblies can be guided using hydrogen bonding,^[8,9] to control and guide new surface phases formed by subsequently deposited molecules.^[4] A highly regular mesh of hexagonal boron nitride has been fabricated recently by self organization on a Rh(111) single-crystalline surface,^[10] this process also leads to ordering of C₆₀ molecules. An alternative approach is to use vicinal surfaces, i.e., surfaces which have small deviations from the most symmetric crystallographic planes. They represent periodic arrays of steps on the nanometer scale with adjustable dimensions, and thus are of great interest for the fabrication of arrays of nanowires^[11–13] or dots.^[14,15]

The C₆₀ molecule has attracted considerable attention because of its remarkable stability, its potential application as an acceptor unit in photovoltaic devices, and as a unique platform for supramolecular chemistry.^[16,17] Ordered layers of C₆₀ can be used as templates for additional deposition due to their higher corrugation, when compared with atomic surfaces.^[18] Polymerization of C₆₀ layers on surfaces is of considerable interest concerning the use of fullerenes as material-resistive masks for high-resolution photolithography.^[19]

Here we report on an easy-to-prepare, self-organized array of fullerene islands on a stepped gold surface. Self-organized, two-dimensional (2D) C₆₀ islands occur on Au(788) and form a well-ordered rectangular array extending over distances of hundreds of nanometers and covering almost the entire crystal surface. The high quality of this periodic structure together with its easy fabrication render this adsorption system a promising candidate for directing further deposition of functional units.

The use of vicinal Au(788) was motivated because of its a priori (2D) periodic patterning.^[14] This surface consists of a periodic succession of {111} minifacets separated by 3.9 nm wide (111) terraces. The terraces are reconstructed with the discommensuration lines perpendicular to the step edges, separating face-centered cubic (fcc) and hexagonal close-packed (hcp) stacking fault domains with a periodicity of 7.2 nm. Step edges and discommensuration lines together represent a regular periodic pattern all over the sample (Fig. 1a, the direction of ascending steps runs from the bottom left of the image to its top right). Room-temperature deposition of C₆₀ at very low coverage on the Au(111) surface was shown to lead to an adsorption only on step-edge fcc segments.^[20,21] Consequently, the Au(788) surface seemed to serve as a promising template to realize an ordered array of C₆₀ nanostructures. Regular meshes of Co islands with lateral extensions of the order of 100 nm were reported previously.^[14]

Figure 1b shows a pseudo three-dimensional (3D) view of a constant-current scanning tunneling microscopy (STM) image

[*] Dr. J. Kröger, Dr. N. Néel, Prof. R. Berndt
Institut für Experimentelle und Angewandte Physik
Christian-Albrechts-Universität zu Kiel
D-24098 Kiel (Germany)
E-mail: kroeger@physik.uni-kiel.de

[**] We are grateful to J. E. Ortega (Universidad del País Vasco, Spain) and C. Cepek (Laboratorio Nazionale TASC, Italy) for providing the Au(788) sample and clean C₆₀ molecules. We acknowledge financial support by DFG through the ESF SONS program.